Multiscale Modeling of Precipitate Microstructure Evolution

V. Vaithyanathan,[1] C. Wolverton,[2] and L. Q. Chen[1]

[1]*Department of Materials Science, Pennsylvania State University, University Park, Pennsylvania 16802*
[2]*Ford Research Laboratory, MD3028/SRL, Dearborn, Michigan 48121-2053*

We demonstrate how three "state-of-the-art" techniques may be combined to build a bridge between atomistics and microstructure: (1) first-principles calculations, (2) a mixed-space cluster expansion approach, and (3) the diffuse-interface phase-field model. The first two methods are used to construct the driving forces for a phase-field microstructural model of θ'-Al$_2$Cu precipitates in Al: bulk, interfacial, and elastic energies. This multiscale approach allows one to isolate the physical effects responsible for precipitate microstructure evolution.

The structure of a material exhibits fluctuations on a variety of length scales. At the angstrom scale, atomic scale fluctuations predominate, while macroscopic defects such as scratches are visible to the naked eye. Intermediate between these two extremes, fluctuations of a material's structure on the micron length scale are often directly tied to its mechanical properties. Thus, understanding microstructure and its evolution is intimately linked to explaining a material's properties during processing. For example, commercial alloys are often aged at elevated temperatures to increase their strength. The structural cause of the hardening is the formation of precipitates which can have sizes typically ranging from 1 nm–1 μm. Current microstructure models, which can be used to optimize a material's properties, are often highly empirical. A more predictive first-principles approach to modeling microstructures would represent an important advance both in terms of the scientific understanding necessary to construct such a model and also in terms of its practical impact.

Although highly accurate for predicting alloy properties of stable and metastable phases, current computational resources limit density functional calculations to relatively small systems with a few hundred atoms. Therefore, the *direct* application of these techniques to problems of alloy microstructure (involving billions of atoms or more) is clearly inaccessible. On the other hand, continuum phase-field models have been successful at accurately describing alloy microstructure evolution; however, these methods are formulated in terms of empirical or difficult-to-measure thermodynamic input. Compounding the difficulty in obtaining a quantitative thermodynamic description of precipitates is that phases of interest are often metastable. Here, we show how first-principles atomistics may be brought together with a continuum phase-field model, with the mixed-space cluster expansion (MSCE) serving as an intermediate tool to bridge from angstroms to microns. With this multiscale tool we study the problem of θ'-Al$_2$Cu evolution in an Al matrix and demonstrate that we can clarify a long-standing debate about the physi-

cal contributions to the energetics responsible for ultimate precipitate morphology.

Two-phase microstructure can be represented by field variables (e.g., composition and long-range order parameters) that distinguish the parent and product phases. The idea embodying the diffuse-interface phase-field description is to make the field variables spatially inhomogeneous and continuous. Though the microstructure evolution in reality is a three dimensional problem, our simulation is in two dimensions (2D) because realistic cell sizes in three dimensions (3D) are computationally prohibitive. For precipitation of tetragonal θ'-Al$_2$Cu in an fcc Al solid solution (SS), the microstructural description requires three field parameters in 2D: solute concentration (c) and two order parameters ($\eta_p; p = 1, 2$). While c represents the compositional differences between the matrix and precipitates, η_p represents the structural differences and also distinguishes the two orientational variants of the precipitates. The thermodynamics of the phase transformation and the accompanying microstructure evolution is modeled by a free energy functional which can be separated into the following three contributions:

$$F_{\text{tot}} = F_{\text{bulk}} + F_{\text{inter}} + F_{\text{elast}}, \tag{1}$$

where F_{bulk} is the bulk free energy, F_{inter} is the interfacial free energy, and F_{elast} is the coherency strain energy arising from the lattice accommodation along interfaces in a microstructure. The first two contributions to the free energy may be written as

$$F_{\text{bulk}} + F_{\text{inter}} = \int_V \left\{ f[c(\vec{r}), \eta_p(\vec{r})] + \frac{\alpha}{2} |\nabla c(\vec{r})|^2 \right. $$
$$\left. + \frac{1}{2} \sum_{p=1}^{2} \beta_{ij}(p) \nabla_i \eta_p(\vec{r}) \nabla_j \eta_p(\vec{r}) \right\} dV \tag{2}$$

where $f(c, \eta_p)$ is the local free energy density [1] and α and $\beta_{ij}(p)$ are the gradient energy coefficients which control the width of the diffuse interface. The strain energy is obtained from elasticity theory using the homogeneous modulus approximation (see Ref. [2]).

With the total free energy expressed as a function of field variables, the temporal evolution of microstructure during a phase transformation is obtained by solving the coupled Cahn-Hilliard equation for c, and the time-dependent Ginzburg-Landau equation for η_p:

$$\frac{\partial c}{\partial t} = M\nabla^2\left[\frac{\partial f}{\partial c} - \alpha\nabla^2 c\right], \tag{3}$$

$$\frac{\partial \eta_p}{\partial t} = -L(\hat{\phi}_p)\left[\frac{\partial f}{\partial \eta_p} - \beta_{ii}(p)\nabla_i^2\eta_p + \frac{\delta E_{el}}{\delta \eta_p}\right], \tag{4}$$

where M is solute mobility in SS and L is the constant associated with interface kinetics $[M/(L\Delta x^2) = 1$, where Δx is the grid spacing; we found that the quantitative precipitate morphology remains the same for $M/(L\Delta x^2) = 1$ to 100]. L is expressed as a function of $\hat{\phi}_p$, the normal to the precipitate interface $(\hat{\phi}_p = \vec{\nabla}\eta_p/|\vec{\nabla}\eta_p|)$, to include the significant kinetic anisotropy observed from experiments on lengthening and thickening kinetics [3,4].

As the discussion above illustrates, the continuum phase-field methodology relies on three energetic quantities as input: (i) bulk free energies of solid solution and precipitate phases, (ii) precipitate-matrix interfacial free energies, and (iii) precipitate/matrix lattice parameters and elastic properties. Experimental determination of these quantities can be problematic. What is required to make the phase-field calculations more predictive in nature is a physically motivated method for accurately obtaining these input quantities. We show that a combined first-principles/statistical mechanics approach can be used to construct the three energetic contributions to the free energy in Eq. (1).

Our first-principles calculations are based on density functional theory within the local density approximation. For total energy calculations, we use both the full-potential linearized augmented plane wave method (FLAPW) [5] and the pseudopotential method utilizing ultrasoft pseudopotentials as implemented in the Vienna *ab initio* simulation package (VASP) [6]. Vibrational entropies were taken from the linear response calculations in Ref. [7], which utilized norm-conserving pseudopotentials. Careful tests were performed to ensure that the energetics were converged with respect to **k** points (up to a $16 \times 16 \times 16$ grid was used) and basis-set cutoffs (up to $E_{cut} = 16.7$ and 21.5 Ry were used in the FLAPW and VASP calculations, respectively). In all cases, structures were fully relaxed with respect to volume as well as all cell-internal and cell-external coordinates [8].

Bulk free energies.—Although much simpler than the computation of a full microstructural morphology, the calculation of the free energy of a disordered solid solution phase is still outside the realm of *direct* first-principles applications, due to the disorder involved as well as the configurational entropy contribution. However, a tool does exist which makes possible the extension of first-principles energetics to solid solution phases at finite temperatures including full atomic relaxations: the MSCE

[9]. In the MSCE technique, energetics of small unit cell ordered compounds are mapped onto a generalized Ising-like model for a particular lattice type, involving 2-, 3-, and 4-body interactions plus coherency strain energies. The Hamiltonian can be incorporated into mixed-space Monte Carlo simulations of $N \sim 10^5$ atoms [10], effectively allowing one to explore the complexity of the 2^N configurational space. An MSCE of fcc Al-Cu energetics has been constructed [10] from first-principles energetics of ~ 40 ordered structures combined with coherency strain calculations. Using this MSCE in Monte Carlo simulations, coupled with thermodynamic integration, we obtain the bulk free energy of the disordered Al-Cu solid solution phase, as shown in Fig. 1 at several temperatures. The Al-Cu MSCE is applicable only to substitutional fcc-based configurations and hence is not amenable to determine properties of θ' which has a (distorted) CaF_2 crystal structure. For these properties, rather than a MSCE, we appeal to direct first-principles calculations: The free energy of θ' is obtained from first-principles calculations of the $T = 0$ K energetics, coupled with the calculated vibrational entropy of this phase which has recently been found to be unexpectedly important in this system [7,11]. Bulk defect (antisite and vacancy) energies of θ', calculated via first-principles supercell energies, are quite large, consistent with a line compound description.

The combination of (i) first-principles total energies, (ii) linear response calculations, (iii) the MSCE approach, (iv) Monte Carlo simulations, and (v) thermodynamic integration yields the bulk free energies of matrix and precipitate phases. These bulk free energies are used to fit the coefficients of coarse-grained free energy polynomial [1]
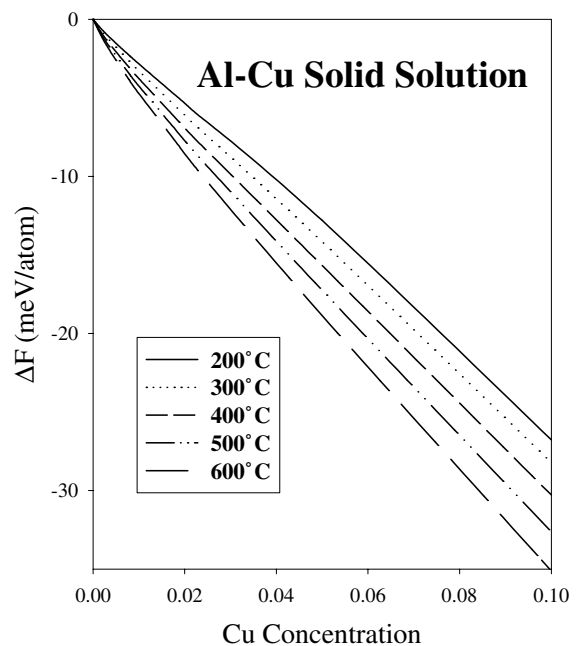

FIG. 1. Free energy of an Al-Cu solid solution, calculated from a first-principles MSCE combined with thermodynamic integration of Monte Carlo results.

in c and η. The form of the coarse-grained polynomial is based on the symmetry requirements of the transformation. To enable direct calculation of the free energy from first principles, we assume that the long-range order parameters are "slaved" by the composition; i.e., the order parameters are at equilibrium for a given composition.

Interfacial energies.—In a perfectly coherent precipitate-matrix system, one could calculate the interfacial free energies from a Monte Carlo simulation coupled with thermodynamic integration, analogous to the procedure described above for bulk free energies. Alternatively, $T = 0$ K values may be obtained from direct first-principles supercell calculations (i.e., without the need for a CE). Because the problem of θ' precipitation involves partially coherent precipitates with different crystal structures for precipitate and matrix, it is not amenable to the CE method, and therefore we limit ourselves to $T = 0$ K interfacial energies from direct first-principles calculations. It has been experimentally shown that θ' precipitates form partially coherent (001) plates, with coherent $(001)_{\theta'} \parallel \{001\}_{Al}$ interface on the broad faces of the plates, and semicoherent [12] interfaces around the rim of the plates, a portion of which are $(100)_{\theta'}$ and $(010)_{\theta'} \parallel \{100\}_{Al}$ [3]. These coherent and semicoherent interfaces possess very different interfacial structures (see Fig. 2): across the coherent interface, the lattice parameters are comparable and hence the interfacial structure is represented as a $1a_{\theta'} = 1a_{Al}$ unit cell. The interfacial structure across the semicoherent interface can have different combinations of θ':Al unit cells. The most commonly observed structure at small θ' thicknesses is a $2c_{\theta'} = 3a_{Al}$ configuration [13] (also see below).

The Al/θ' interfacial supercells are shown in Fig. 2. Interfacial energies are obtained from VASP calculations of these supercell energies, by subtracting the bulk energies of θ' and Al, accounting for coherency strain effects. Supercells with 24 to 120 atoms were used, with the large
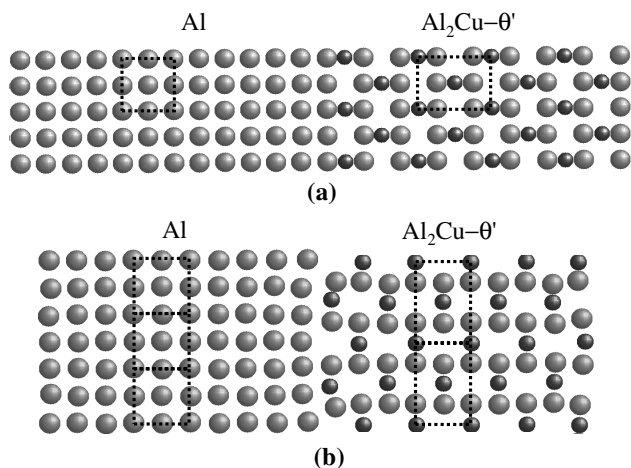

(a)

(b)

FIG. 2. Relaxed supercells used to calculate Al$_2$Cu(θ')/Al interfacial energies for both (a) the coherent (100) interface and (b) the "semicoherent" (001) interface. Dashed lines indicate the $1a_{\theta'} = 1a_{Al}$ and $2c_{\theta'} = 3a_{Al}$ relationships of the coherent and semicoherent interfaces, respectively.

supercell results demonstrating that the energies are well converged with respect to supercell size. The calculated $T = 0$ K first-principles interfacial energies for coherent and semicoherent interfaces are 235 and 615 mJ/m^2, respectively. Interestingly, a semicoherent interfacial energy of similar magnitude was predicted by the simple calculations of Aaronson and Laird [14] with an interfacial energy anisotropy of ~ 12 for θ' precipitates, often quoted in the literature as an estimate of the equilibrium aspect ratio. However, our (much more accurate) first-principles calculations demonstrate that the anisotropy is actually closer to ~ 3, and we use these values along with the bulk free energies to determine the (concentration-independent) gradient energy coefficients of Eq. (2), using the expression of Cahn and Hilliard [15] which interrelates these quantities.

Elastic strain energies.—The interfacial energies and the strain induced by lattice mismatch are not independent quantities, as a large mismatch strain may be partially alleviated by incoherency in the interface, which in turn will increase the interfacial energy. The atomic scale details of precipitate interfaces and morphology is determined by the delicate balance between these two effects. To obtain the elastic energy, one must know the elastic constants of θ'-Al$_2$Cu. These values are not known experimentally but were calculated for cubic (CaF$_2$)θ' via FLAPW (C$_{11}$ = 1.9 Mbar, C$_{12}$ = 0.8 Mbar, and C$_{44}$ = 0.9 Mbar). The elastic anisotropy C$'$-C$_{44}$ = −0.35 Mbar < 0 indicates an elastically soft $\langle 100 \rangle$ direction for θ'. The elastic moduli input to the phase-field model is taken from a balance of the first-principles calculated C$_{ij}$ of θ' and fcc Al [9], yielding C$_{12}$/C$_{11}$ = 0.442 and C$_{44}$/C$_{11}$ = 0.428, for a volume fraction of 5% θ'. These values, along with the calculated lattice parameters of each phase, provide the necessary parameters for elastic energy calculations in the phase-field model. The lattice strains obtained from calculations, with interfacial structures of $1a_{\theta'} = 1a_{Al}$ and $2c_{\theta'} = 3a_{Al}$ for coherent and semicoherent interfaces, are +0.68% and −5.1%, respectively. The experimental observation [13] of the $2c_{\theta'} = 3a_{Al}$ unit cells configuration can be understood by its ability to form the least strained interface with one of the smallest integral unit cells combination. (Misfit strains for a few $nc_{\theta'} = ma_{Al}$ unit cells combination, n, m are positive integers, are (i) $1c_{\theta'} = 1a_{Al}$—+43%, (ii) $1c_{\theta'} = 2a_{Al}$—−28.7%, (iii) $2c_{\theta'} = 3a_{Al}$—−5.1%, and (iv) $3c_{\theta'} = 4a_{Al}$—+6.9%.) Thus our results demonstrate that *both* interfacial and elastic anisotropies favor the observed plate morphology of θ'.

We have obtained all of the necessary thermodynamic input for the microstructural evolution of this system from an atomistic, predictive methodology. Incorporating these energetics in Eq. (1), we compute the temporal evolution of microstructure via Eqs. (3) and (4), resulting in a multiscale model of precipitate evolution (Fig. 3).

For *small* precipitates ($\lesssim 10$ nm [16]), the equilibrium shape is governed by interfacial energies. Our calculations suggest that small θ' particles (e.g., the θ' nuclei) will
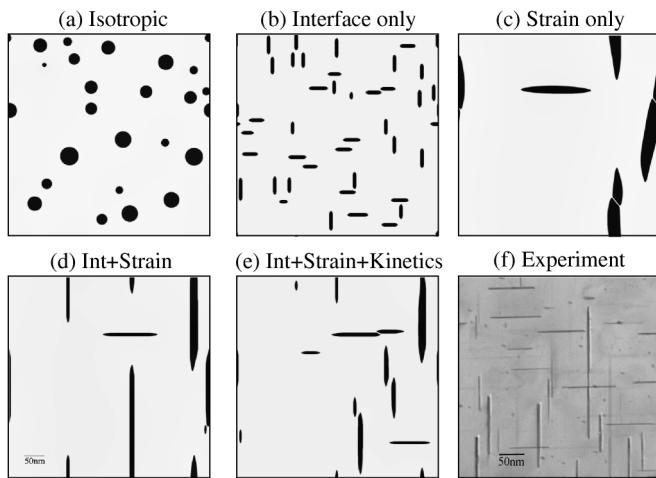
FIG. 3. Phase-field simulation using thermodynamic parameters from first principles, showing θ' morphologies obtained with different anisotropic contributions ($T = 450\,°\mathrm{C}$ was used in all simulations [11]). The experimental micrograph is an Al-Si-Cu cast alloy aged at $230\,°\mathrm{C}$ for 3 h. The label on the top of each frame indicates the anisotropy(ies) included (expressed as semicoherent:coherent; Interface—~3:1, Strain—$-0.051:+0.0068$; "extrinsic" Kinetics—1:0.01).

adopt an aspect ratio based on the interfacial anisotropy, or ~3:1. We therefore nucleate precipitates in our phase-field model by starting with a random distribution of θ' particles with aspect ratios ~3:1. Our model contains anisotropies in both interfacial energies and coherency strain (obtained from first principles and the MSCE). These thermodynamic driving forces will lead to an "intrinsic" kinetic anisotropy in the coherent and semicoherent interface growth kinetics in the model. In addition, the different interface migration mechanisms (e.g., ledge growth vs diffusion controlled) and the presence of short circuit diffusion paths which have been extensively discussed in the literature [3,4] may also lead to an additional "extrinsic" kinetic anisotropy. We can incorporate this extrinsic anisotropy in the phase-field model artificially via $L(\hat{\phi}_p)$ in Eq. (4). By systematically suppressing or activating the various anisotropies (interfacial energy, strain, and extrinsic interfacial kinetics) we are able, for the first time, to clarify the *physical contributions* responsible for the observed morphology of θ' precipitate microstructure. In Fig. 3, we compare the θ' morphologies obtained from our multiscale simulation (with various anisotropic contributions) with an experimental micrograph from an industrial Al-Si-Cu cast alloy. The generic plate shape can be produced by any of the anisotropic effects, but *a comparable aspect ratio is obtained only with the combination of both interfacial and elastic anisotropies*. All the simulation figures are drawn to the same length scale indicated in Fig. 3(d).

Another important aspect of the simulated microstructure obtained from our multiscale model compared to other phase-field simulations is that the predictions are

quantitative and not just qualitative. The calculated precipitate dimensions and aspect ratios are similar in magnitude to the experimental measurements. A more detailed account of the quantitative growth kinetics, precipitate dimensions, composition dependencies, etc. from our model is forthcoming. This type of physics-based multiscale first-principles/phase-field approach should be generally applicable to a wide variety of microstructural problems.

[1] D. Y. Li and L. Q. Chen, Acta Mater. **46**, 2573 (1998).
[2] A. G. Khachaturyan, *Theory of Structural Transformations in Solids* (John Wiley, New York, 1983).
[3] H. I. Aaronson and C. Laird, Trans. Metall. Soc. AIME **242**, 1437 (1968).
[4] R. Sankaran and C. Laird, Acta Metall. **22**, 957 (1974).
[5] D. J. Singh, *Planewaves, Pseudopotentials, and the LAPW Method* (Kluwer, Boston, 1994).
[6] G. Kresse and J. Furthmüller, Comput. Mater. Sci. **6**, 15 (1996).
[7] C. Wolverton and V. Ozolins, Phys. Rev. Lett. **86**, 5518 (2001).
[8] The combination of different first-principles energies into a single microstructural model might initially cause concern; however, we tested the formation energies of more than 20 different fully relaxed ordered compounds of Al-Cu with both the FLAPW and VASP methods. The average deviation between the two methods energies is extremely small (~6 meV/atom out of average formation energies of more than 100 meV/atom), thus inspiring confidence that the FLAPW/VASP energies are basically interchangeable for this system.
[9] D. B. Laks, L. G. Ferreira, S. Froyen, and A. Zunger, Phys. Rev. B **46**, 12 587 (1992).
[10] C. Wolverton, Philos. Mag. Lett. **79**, 683 (1999).
[11] Currently, we have not computed the vibrational entropy contribution to the disordered solid solution phase. This approximation serves mostly to decrease solubility and hence leads to an overestimate of the temperature scale, as has recently been shown in Al-Sc alloys [V. Ozolins and M. Asta, Phys. Rev. Lett. **86**, 448 (2001)]. Comparing our data with the Al-Cu phase diagram shows a ~$200\,°\mathrm{C}$ overestimate of temperature.
[12] A semicoherent interface has misfit dislocations interspersed along the interface.
[13] W. M. Stobbs and G. R. Purdy, Acta Metall. **26**, 1069 (1978).
[14] H. I. Aaronson and C. Laird, Ford Motor Co. Scientific Laboratory Report No. SL 67-52, 1967.
[15] J. W. Cahn and J. E. Hilliard, J. Chem. Phys. **28**, 258 (1958).
[16] D. Mitlin, V. Radmilovic, and J. W. Morris, Jr., Metall. Mater. Trans. **31A**, 2697 (2000).